How Does a Thin Wetted Film Dry Up?

M. Elbaum and S.G. Lipson
Physics Department, Technion-Israel Institute of Technology, 32000 Haifa, Israel
(Received 20 October 1993)

We study the thinning by evaporation of completely wetted water films on clean mica surfaces in a pure water vapor environment. In the thickness range from 100 to approximately 1000 Å the thinning is unstable to nucleation of dry patches, and the spreading of these patches invokes a "dewetting" of the substrate. The initial process is described by a simple nucleation theory. A number of hydrodynamic effects and instabilities are also observed at the boundary of the film.

PACS numbers: 68.15.+e, 47.20.Dr, 82.60.Nh

Thermodynamically, the simple process of drying a thin liquid film from a wetted substrate might be considered the reversible counterpart to wetting, which enjoys a broad and well-developed literature [1–3]. In the case of *complete* wetting, a saturated condensable vapor spontaneously forms a uniform continuous film with zero contact angle on a substrate to which is exposed [4]. If the vapor pressure is then reduced below saturation, the film should simply thin. The stability of thin films is itself an active topic, but the literature concentrates on rupture of free or nonwetting films [5–10]. Brochard-Wyart and Daillant [11] have proposed the possibility that dewetting occurs by the nucleation and spreading of dry patches in the film even for the case of complete wetting, though with the restriction to nonvolatile fluid materials. Here we report experimental results demonstrating nucleated dewetting, driven by evaporation, of a thin film of supercooled water from a completely wetted mica substrate. We explain the observations in terms of a simple classical nucleation model, intended to complement the hydrodynamic treatment of Ref. [11]. In essence it is understood as a substrate-mediated boiling phenomenon in two dimensions.

Two important experimental works on dewetting [12,13] have followed from Brochard-Wyart and Daillant's theory. In both cases the fluids were nonvolatile materials on nonwetted substrates. Films were spread mechanically by dragging or spinning. Such a film is unstable and would be expected to remove itself spontaneously by a nucleation process. Because of conservation of fluid volume the final stage of the breakup is an array of droplets, with some hydrodynamically determined characteristic size. Measurements of the spreading velocity of the drying front [12], and the size and spacing of the final droplets [13], are in agreement with theory. The theory also treats the case of a wetted substrate, again conserving fluid volume by restriction to nonvolatile fluids; the film is unstable if its thickness is below a critical value equal to the ultimate thickness of the film to which a droplet would spread, the so-called "pancake" of de Gennes [2].

Our case is entirely complementary to the above. We study a *volatile* fluid, water, on a *completely wettable* substrate of freshly cleaved mica. The experiment is conducted entirely in a temperature-controlled vacuum chamber filled with pure water vapor at controllable pressure. A condensing film wets the mica with zero contact angle. During evaporation, dewetting may nonetheless occur by nucleation and spreading of dry patches, inside of which the film thickness should equal the value which would be reached in an equilibrium adsorption experiment at the imposed subsaturation, typically tens of angstroms. In the final film-vapor equilibrium, the entire film should be reduced to this value.

The apparatus consists of two well-insulated copper chambers with independent temperature control. They are attached to each other by a tube with a valve, and individually to a gas handling manifold with double LN2-trapped mechanical and mercury diffusion pumps. Ice is condensed into one chamber by distillation from a source flask of water at room temperature, previously degassed by repeated pumping and freezing. This provides a vapor source at constant pressure P_1 determined by the "source" chamber temperature T_1. Inside the second chamber is a smaller evacuated cell containing a sealed copper disk sitting on a small thermoelectric cooler. A precision thermistor sits in a hole drilled near the upper surface of the disk. On top of the copper disk a thin plate of mica (~ 50 μm thickness) is attached by means of graphite-loaded high vacuum grease. The graphite loading improves the thermal conductivity of the grease and optically darkens it. We cleave the mica in air immediately before closing the chamber. (A delay here would permit the development of undesired hydrophobicity, which was occasionally observed.) This whole assembly sits under an optical window in the cover. The second chamber is held initially at a slightly higher temperature than the source to prevent the formation of ice on its interior walls. All the measurements reported here are made with deeply supercooled water, at temperatures as low as $-30\,^{\circ}$C. This has the effect of increasing both the viscosity and the surface tension above their familiar room temperature values, as well as demonstrating the cleanliness of the system.

0031-9007/94/72(22)/3562(4)$06.00

Condensation is induced on the mica by cooling it. The vapor pressure P_1 equals the saturated vapor pressure over a bulk quantity (or thick film) of supercooled water at temperature $T_2^* < T_1$. A liquid film at such a temperature and pressure, on a wettable substrate, is stable at any bulk thickness. Condensation is induced by cooling below T_2^*, evaporation by warming above T_2^*. At the temperature of the film the imposed vapor pressure P_1 represents a super- or subsaturation, respectively.

Observations are made optically using thin-film interference with incident light microscopy and monochromatic illumination at λ_0=5896 Å. The image from the substrate and film is captured by a black-and-white charge coupled device video camera and recorded onto video cassettes. When a film of quarter-wavelength optical thickness appears on the mica, the normal incidence reflectivity is reduced by destructive interference to its minimal value. This occurs at a physical thickness of 1107 Å. Thinner films are resolved by quantitative analysis of intensities and comparison to the squared sinusoidal dependence of reflected intensity with thickness.

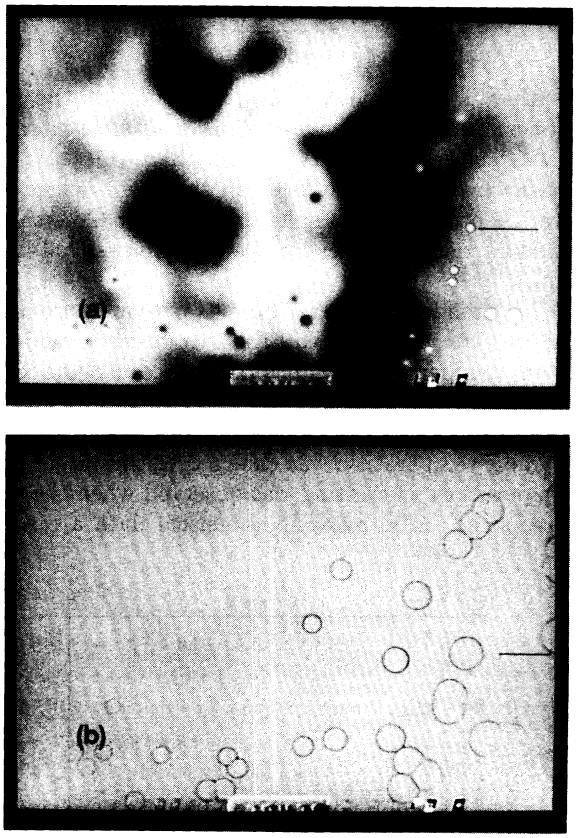

FIG. 1. A film thinning by evaporation begins to "dewet" by the nucleation of circular dry patches (a). The patches spread as the surrounding film thins (b). The rims surrounding dry patches thicken, however, leaving a network of unstable annuli before final evaporation. The sample temperature is −30.4 °C. The patch indicated by the dark line is analyzed in Fig. 2.

In Fig. 1 we show a typical pattern of dry patches nucleated from a thinning film. The time interval between the images is 12 s. In Fig. 2 we show an optical intensity profile taken horizontally across one patch along its diameter. It is clear that the adjoining film is thicker to the left of the patch than to the right, yet the shape is circular; thus the surface tension at the edge dominates in determining the shape. (In other observations we saw a uniform thinning film, also with circular dry patches.) The diameter of the patch grows linearly with time, as can be seen directly from Fig. 2. The thickness of the film remote from the expanding patch decreases linearly in time.

Brochard-Wyart and Daillant make a number of predictions relevant to the observations reported here. We address them with caution as we have broken the condition of conservation of liquid volume. First, they predict that the rate of increase of the dry patch diameter should decrease in time as $t^{-1/2}$. This is not borne out by our observations. All patches analyzed spread with a linear time dependence until breakup, and within a given run the velocity was the same from patch to patch. Second, Fig. 2 of Ref. [11] shows a schematic profile of a broad rim at the edge of a patch. We observe this rim clearly. However, its shape evolves more quickly than the expansion of the dry patch, in contradiction to the assumption of Ref. [11]. The rim is apparent in the "wings" around the patch indicated in the earliest time profiles of our Fig. 2, and can be seen in the photographs of Fig. 1. At later times this rim becomes unstable to oscillations in its thickness, and the abrupt halt to spreading of the patch coincides with the final collapse of the rim and its breakup into droplets.

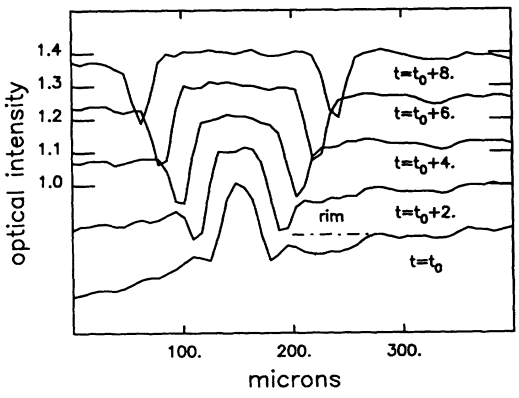

FIG. 2. An intensity profile through one droplet at two-second intervals shows the spreading of the dry patch. The successive curves are offset by 0.1 intensity units for clarity. The diameter of the patch increases linearly in time. A broad "rim" is indicated past the edge of the patch in the two earliest curves; it collapses rapidly into the edge. Note that the intensity at the edge of the patch cannot be interpreted for thickness due to the high curvature there.

A rich series of hydrodynamic phenomena come into play at the rim of the patch. When a dry patch first opens one might expect to see a receding contact angle connecting the surrounding film smoothly and gradually to a film of molecular thickness remaining in equilibrium with the subsaturated vapor pressure. This is not observed. Instead the receding edge disconnects from the substrate and rolls up quickly into a cylinder many times the thickness of the film, under the effect of the Laplace pressure in the highly curved region. Unable to force liquid into the thin viscous film behind, it feeds itself from the film through which it sweeps, simultaneously losing mass by evaporation. The toroidal rim, all the while expanding, is then unstable to axial capillary oscillations leading to its collapse. Figure 3 shows this process in progress.

We now turn to a thermodynamic treatment of the nucleation problem in dewetting. An initial film of thickness l_0, greater than the range of long-ranged interfacial forces, is in coexistence with the vapor above when the chemical potentials of the two phases are equal. The imposition of a chemical potential difference $\Delta\mu = \mu_L - \mu_V > 0$ drives evaporation. At the same $\Delta\mu$, a film of thickness l_1 is stabilized by a disjoining pressure characterizing the complete wetting. We write the free energies:

$$G_{\text{thick}} = A[l_0\rho_L\Delta\mu + \sigma_{SL} + \sigma_{LV} + f(l_0)], \quad (1)$$

$$G_{\text{thin}} = A[l_1\rho_L\Delta\mu + \sigma_{SL} + \sigma_{LV} + f(l_1)], \quad (2)$$

where A is a unit area, ρ_L is the density of the liquid, σ terms are bulk surface tensions between solid (S), liquid (L), and vapor (V) phases. We have made the approximation that $\rho_L \gg \rho_V$. $f(l)$ is the free energy contribution due to interactions across the thin film, for example van der Waals forces varying as l^{-3}. It is positive and monotonically decreasing for complete wetting. The thick film is beyond the range of $f(l)$, i.e., essentially bulk liquid, so that $f(l_0) = 0$. For the thin film this term cancels the first term involving $\Delta\mu$, leaving $G_{\text{thin}} = A[\sigma_{SL} + \sigma_{LV}] = A\sigma_{SV}^{\text{wet}}$, to give zero spreading pressure in equilibrium.

A film with a single hole of radius x has the free energy:

$$G_{\text{hole}} = (A-\pi x^2)[l_0\rho_L\Delta\mu + \sigma_{SL} + \sigma_{LV}] + \pi x^2\sigma_{SV}^{\text{wet}} + 2\pi x(l_0 - l_1)\sigma_{LV}. \quad (3)$$

The last term represents the cost of creating the extra surface at the cylindrical wall surrounding the hole. The free energy difference $\Delta G = G_{\text{hole}} - G_{\text{thick}}$ reduces quite simply to

$$\Delta G = -\pi x^2 l_0\rho\Delta\mu + 2\pi x l_0\sigma_{LV}. \quad (4)$$

The critical hole radius and free energy barrier are found at the point where $\partial\Delta G/\partial x = 0$:

$$x^* = \frac{\sigma_{LV}}{\rho_L\Delta\mu}, \quad (5)$$

$$\Delta G^* = \frac{\pi l_0\sigma_{LV}^2}{\rho_L\Delta\mu}. \quad (6)$$

Note that x^* is exactly half the radius of the critical sphere in ordinary three-dimensional nucleation, and that ΔG^* varies as $l_0\sigma^2/\Delta\mu$ rather than $\sigma^3/(\Delta\mu)^2$ [14]. A crossover occurs when the film thickness reaches 8/3 the radius of the critical sphere; in thinner films the activation barrier is smaller for the two-dimensional mechanism.

We have made a number of quantitative measurements, the results of which lead to Fig. 4. In order to maintain constant temperature conditions, a modified procedure was used for these data. A thick film (≈ 5000 Å) was first prepared, and then with the communicating valve closed, the sample temperature was changed to the target value for evaporation. Dewetting was observed when the valve was reopened. The relevant numerical data are source

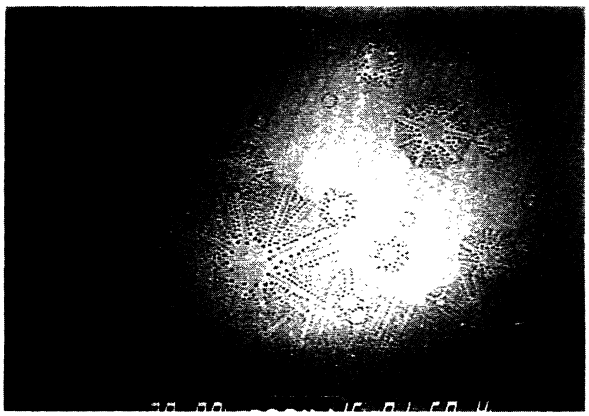

FIG. 3. Following the rupture of the cohesive edge surrounding a patch, the film continues to "dewet," leaving a succession of droplets behind the drying front. Many stages in the process are visible here. The sample temperature is $-30.0\,^\circ$C.

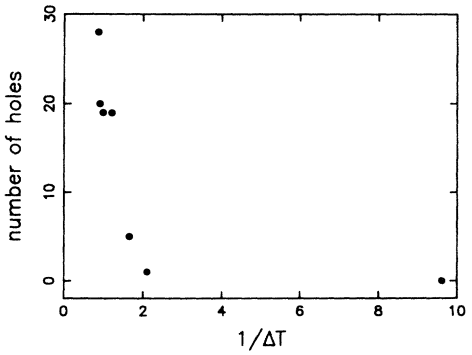

FIG. 4. The number of optically resovable holes nucleated in a selected region of the surface, as a function of temperature imbalance ΔT. The balance temperature $T = -15.7\,^\circ$C.

temperature $T_1 = -15.7\,^{\circ}\mathrm{C}$, ΔT ranging from 0.104 to 1.161. Evaporation rates for thick films under such conditions were 200 to 2100 Å/sec. For thin films (< 500 Å) this rate slowed dramatically, to approximately 1 to 10 Å/sec. If the valve is closed during the process the film rewets, though very slowly compared to the dewetting. Similarly, if T_2 is lowered following dewetting, the film rewets with no advancing contact angle.

We translate the evaporation drive $\Delta\mu$ into the experimentally measured temperature difference between that at which the thick film does not grow or recede relative to the imposed vapor pressure, and the actual (warmer) temperature of the film. Using the chemical potential of the ideal gas and the Arhhenius dependence of vapor pressure on temperature, we get $\Delta\mu = q\Delta T/T$, where q is the heat of evaporation and T is the balance temperature described above. Extrapolating from standard tables [15] for q ($q = 6.8 \times 10^{-13}$ erg/mol), the critical hole radius in angstroms $x^* = 82/\Delta T$ and thus ranges from 790 to 71 Å.

Figure 4 shows the number of holes sufficiently large to be resolved optically which nucleated in a selected region of the surface, approximately 5 mm^2 in area, plotted vs $1/\Delta T$. The dependence is clearly activated. However, our inability to detect holes of a size comparable to x^* makes it impossible to determine a meaningful activation energy. There is little direct evidence for heterogeneous nucleation by defects or impurities since we only rarely observed patches nucleating repeatedly in the same positions.

In summary, we have presented experimental evidence of nucleated dewetting of volatile water films on a substrate which has been completely wetted by direct vapor adsorption. The nucleation of holes in the film is modeled as a substrate-mediated boiling. Connection has been made with nucleated dewetting of nonvolatile, nonwetting films, where the departure from equilibrium is imposed by the initial film geometry rather than the externally variable evaporation drive. There is also a qualitative similarity to the nucleated thick-thin transition in Newton black films [16]. The system displays a richness of hydrodynamic effects and instabilities which we will discuss at greater length in future publications.

The authors are most grateful to E. Braun, D. Levine, Y. Avron, and J.S. Wettlaufer for their insights and encouragements. This work was supported in part by grants from the German–Israel Foundation and the Israel Academy of Sciences, and by the Fund for the Promotion of Research at the Technion.

[1] J.G. Dash, *Films on Solid Surfaces* (Academic Press, New York, 1975).
[2] P.J.G. de Gennes, Rev. Mod. Phys. **57**, 827 (1985).
[3] L. Leger and J.F. Joanny, Rep. Prog. Phys. **55**, 431 (1992).
[4] M. Schick, in *Liquids at Interfaces*, Les Houches Session XLVIII, 1988, edited by J. Charvolin, J.F. Joanny, and J. Zinn-Justin (Elsevier, New York, 1990).
[5] E. Ruckenstein and R.J. Jain, J. Chem. Soc. Faraday Trans. 2, **70**, 132 (1974).
[6] M.B. Williams and S.H. Davis, J. Colloid. Interface Sci. **90**, 220 (1982).
[7] D.J. Srolovitz and S.A. Safran, J. Appl. Phys. **60**, 247 (1986); **60**, 255 (1986).
[8] M. Prevost and D. Gallet, J. Chem. Phys. **84**, 4043 (1986).
[9] H.S. Kheshgi and L.E. Scriven, Chem. Eng. Sci. **46**, 519 (1991).
[10] V.S. Mitlin, J. Colloid. Interface Sci. **156**, 491 (1993).
[11] F. Brochard-Wyart and J. Daillant, Can. J. Phys. **68**, 1084 (1990).
[12] C. Redon, F. Brochard Wyart, and F. Rondelez, Phys. Rev. Lett. **66**, 715 (1991).
[13] G. Reiter, Phys. Rev. Lett. **68**, 75 (1992).
[14] J.W. Christian, *The Theory of Transformations in Metals and Alloys* (Pergamon Press, Oxford, 1981), Pt. I, 2nd ed., pp. 418–24.
[15] G.W.C. Kaye and T.H. Laby, *Tables of Physical and Chemical Constants* (Longman Scientific & Technical, Essex, 1986), p. 268.
[16] D. Chowdhury and D. Stauffer, Physica (Amsterdam) **189A**, 70 (1992).

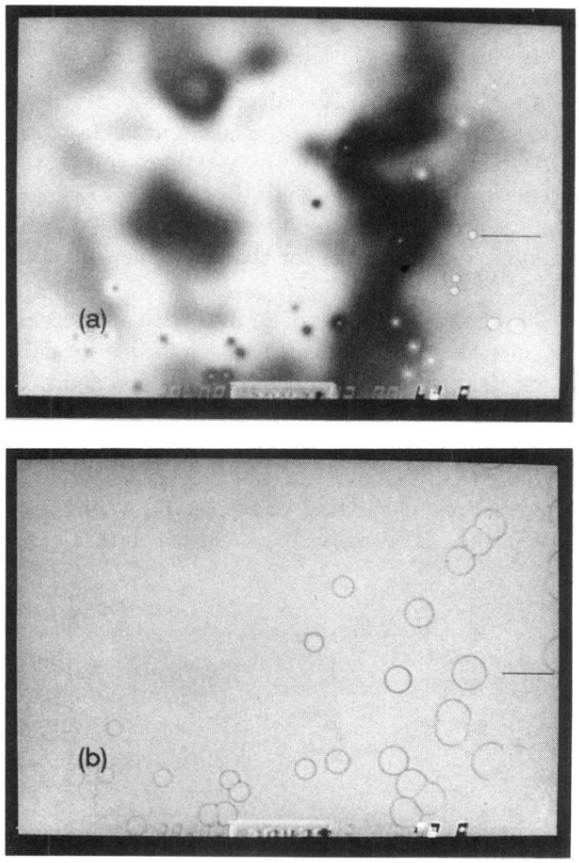

FIG. 1. A film thinning by evaporation begins to "dewet" by the nucleation of circular dry patches (a). The patches spread as the surrounding film thins (b). The rims surrounding dry patches thicken, however, leaving a network of unstable annuli before final evaporation. The sample temperature is $-30.4\,^{\circ}\mathrm{C}$. The patch indicated by the dark line is analyzed in Fig. 2.

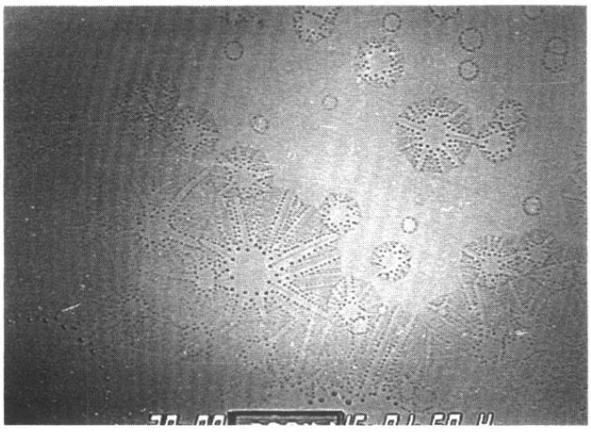

FIG. 3. Following the rupture of the cohesive edge surrounding a patch, the film continues to "dewet," leaving a succession of droplets behind the drying front. Many stages in the process are visible here. The sample temperature is $-30.0\,^{\circ}\mathrm{C}$.